Role of Methylene Diphenyl Diisocyanate (MDI) Additives on SBS-Modified Asphalt with Improved Thermal Stability and Mechanical Performance

Role of methylene diphenyl diisocyanate (MDI) additives on SBS-modified asphalt with improved thermal stability and mechanical performance

Jocelyn H. Ting[#a,b], Eesha Khare[#a,b], Anthony Debellis[e], Brian Orr[c], Jerome S. Jourdan[c], Francisco J. Martín-Martínez[a,d], Kai Jin[a], Bernie L. Malonson[c], Markus J. Buehler[a,*]

a) Laboratory for Atomistic and Molecular Mechanics (LAMM), Department of Civil and Environmental Engineering, Massachusetts Institute of Technology, 77 Massachusetts Ave., Cambridge, MA, 02139 USA.
b) Department of Materials Science and Engineering, Massachusetts Institute of Technology, 77 Massachusetts Ave., Cambridge, MA, 02139 USA.
c) North American Monomers, Analytics North America, BASF Corporation, 1609 Biddle Avenue, Wyandotte, MI, 48192 USA
d) Department of Chemistry, Swansea University, Singleton Park, Swansea, SA2 8PP, United Kingdom
e) BASF Corporation, 540 White Plains Rd, Tarrytown, NY, 10591 USA

#Co-first authors
*Corresponding author: mbuehler@mit.edu

Abstract

Poly (styrene-butadiene-styrene), or SBS, is commonly added to asphalt mixtures to improve their thermal stability and mechanical performance under working conditions in pavements and roads. However, the resulting SBS-modified blend suffers from separation between the SBS polymer and asphalt molecular components, thereby decreasing the expected mechanical performance of the material in the long term. Here we present how adding methylene diphenyl diisocyanate (MDI)-based additives may improve the phase stability of SBS-modified asphalt as measured by AFM and separation testing. We then discuss the fundamental mechanisms that involve SBS, MDI and asphalt molecules to achieve such improvement. To this end, we utilize molecular modeling methods of semi-empirical tight binding, density functional theory, and reaction rate calculations to simulate and characterize the intermolecular interactions of SBS and MDI with asphaltene molecules, a key component of asphalt bitumen. We find that while noncovalent π–π stacking does not significantly explain the macroscopic properties of asphalt blends, reactions between asphaltene and MDI likely occur. As such, we propose that MDI acts as a compatibilizing agent between asphaltenes and SBS, which enhances the phase stability of MDI-SBS-modified asphalt. We also demonstrate that MDI additives with asphalt have lower chemical softness and polarizability, indicating a lower tendency towards degradation by oxidative agents.

Keywords
Methylene diphenyl diisocyanate (MDI), styrene butadiene styrene (SBS), methods (DFT, xTB, AFM), polymer modified asphalt, asphaltene, noncovalent interactions, compatibilizing agent, increased phase stability, lowered oxidative degradation

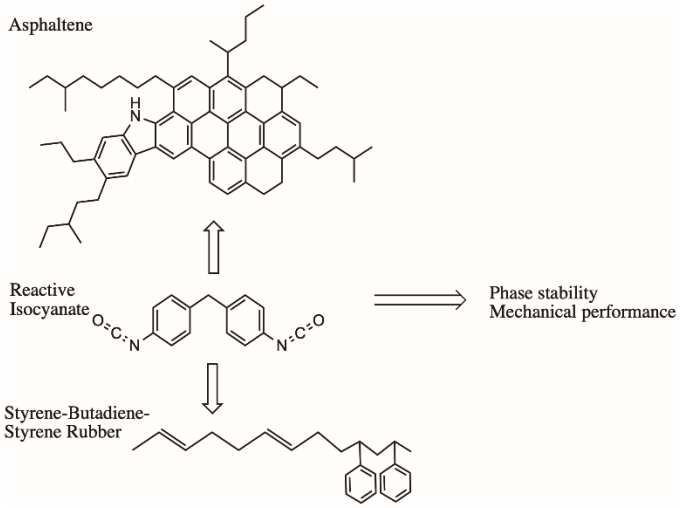

Table of Contents Image

Introduction

Asphalt is commonly used in roads and pavement due to its low cost, relatively easy applicability, and good mechanical performance under loading conditions. However, asphalt properties are challenged when the material needs to perform outside a specific temperature range. At high temperatures, asphalt suffers from rutting, and at low temperatures from cracking. Thus, extending its operational temperature range is necessary to ensure asphalt's reliable performance under changing environmental conditions, different climates and processing parameters. To expand the operational temperature range and to increase the lifetime of asphalt pavement, block copolymer rubbers of poly(styrene-butadiene-styrene), or SBS, are commonly added to the blends, due to SBS temperature stability over a wide range. In addition to this wide temperature stability, SBS rubbers provide excellent stiffness and elastic recovery, arising from a network of glassy polystyrene polymer chains embedded in a rubbery polybutadiene matrix. In fact, it has been found that the addition of even 2.5% of SBS results in an asphalt blend with considerably higher softening point, and higher viscosity, indicating a higher resistance to rutting.[1] Despite these mechanical benefits, SBS-modified asphalt often experiences phase separation at the high temperatures required to pour, store, and transport asphalt (120-200°C).[2–4] This phase separation results in compromised mechanical properties. Since asphalt is not adequately incorporated into the polymer network, the thermal and rheological benefits of the additive are reduced, resulting in failure similar to unmodified asphalt.

To prevent this phase separation between asphalt and SBS, reactive polymers with functional groups capable of binding to asphalt molecules, can be used.[5] Initial studies have found that MDI improves the phase continuity, thermal stability, aging and rutting resistance of SBS-modified asphalt through a variety of proposed chemistries.[6–8] These studies have used FTIR spectroscopy to determine that the isocyanate (–NCO) functional groups of MDI react with hydroxy (–OH) groups in asphalt molecules, for example, asphaltenes, to form urethane linkages.[6] Other studies have also found that adding water to MDI, causes polymerization via urea linkage between MDI monomers [9], which could also occur in when MDI is added to asphalt blends. While initial studies have begun to demonstrate that MDI interacts with asphalt molecules to improved asphalt properties at high temperatures, the exact nature of such interaction is still unknown.[6–8] Therefore, a deeper understanding on two fronts is needed. First, the effect of MDI on the phase stability of asphalt blends needs to be more carefully established. Next, the chemical role of isocyanate functional groups from MDI in stabilizing SBS-modified asphalt mixtures would enable a significant control over the molecular design of asphalt blends that exhibit improved thermal stability and mechanical performance.

To this end, the study reported in this paper combines experimental analysis and molecular modeling of asphalt mixtures to elucidate the role of MDI in stabilizing SBS-modified asphalt. Experimentally, we characterize the structural and rheological properties of commercial asphalt blends mixed with SBS and/or MDI-based additives. Computationally, our models then explore the contribution of noncovalent interactions between MDI functional groups, asphaltene molecules, and SBS functionalities to explain the improved phase and thermal stability that MDI additives provide to SBS-modified asphalts. We isolate the intermolecular interactions that exist between various forms of MDI, the key components of SBS rubber additives, and asphaltene molecules. Asphaltenes are one of the four molecular classes identified by solubility differences in the SARA analysis,[10,11] and a tractable system of study asphalt behavior at the molecular level.

Based on experimental data, a large body of work has been conducted on developing reliable asphalt models.[12–20] From these models, this study focuses on three asphaltene molecules that represent on average the molecular structure and chemical functionalities expected for common asphaltenes.[21–23] The focus on asphaltene molecules within the SARA solubility classes, is also due to the key role that these chemical components play in the formation of molecular aggregates, via in π−π stacking, which leads to clustering and phase separation, significant determinants of the macroscopic mechanical properties of asphalt, as discussed above.[18,20,24,25] For the reactive isocyanate additives, monomeric MDI (4,4'), polymeric MDI (PMDI), and tolyl isocyanate are examined in this study as representative structures.[26] Because MDI can also react with hydroxy functional groups, we include MDI reacted with the –OH group on asphaltenes as well.[6,27]

Rheological and structural properties using dynamic shear rheology (DSR) and atomic force microscopy (AFM) of asphalt blends with various additives are characterized. Semi-empirical tight binding (xTB), density functional theory (DFT), conductor like screening model for real solvents (COSMOtherm) are used to complement this experimental work and computationally characterize the molecular interactions between conformations of additives and asphaltene molecules. The goal of this work is threefold. First, we aim to show that isocyanate additions to SBS-modified asphalt results in similar mechanical properties with no visible phase separation of the asphalt blend. Next, we aim to explain how different types of the MDI additive (monomeric, polymeric, tolyl, and reacted) affect the properties of asphaltene molecules by computing binding energies and reaction rates and suggesting a mechanism whereby MDI stabilizes SBS-modified asphalt through chemical reactions. Last, we briefly discuss how MDI stacked with asphaltenes has a lower chemical softness and polarizability, indicating the likelihood to be less affected by oxidative agents. Our calculations and experiments suggest that reactions with isocyanates play a role in stabilizing SBS-modified asphalt via π−π stacking in some particular molecular arrangements, although other chemical interactions, likely play a large stabilizing role as well.

Experimental and Computational Methods

Asphalt-only (blind sample from unknown Midwest refinery to maintain test integrity), asphalt modified with 2% SBS, a commercial reactive isocyanate-based asphalt provided by BASF,[28–30] and asphalt modified with 2% SBS and 2% reactive isocyanate provided by BASF were characterized.

Separation testing (ASTM D-7173) was performed. Polymer-modified asphalt was prepared by conditioning the sample in a sealed aluminum tube for 48 h at a temperature of 163°C. At the end of the conditioning period, the top and bottom portions are separated and tested using a dynamic shear rheometer (DSR) Anton Paar SmartPave 102 at 64°C to measure dynamic shear modulus and phase angle in accordance with ASTM D7175.

A Multimode 8 and Nanoscope V AFM (Bruker Nano Surfaces, Santa Barbara, CA) was used to characterize asphalt samples to determine if additives can be characterized and if commercial reactive isocyanates affect formation of microstructures in asphalt. TAP525 probes (brukerafmprobes.com) having a high spring constant (k~200N/m) were used to image surfaces of 1 μm thin sections of asphalt that were cooled to < 0°C and microtomed with a diamond knife. The stiff probes were operated at high drive amplitudes and light tapping in order to image the

soft, sticky surfaces with minimal distortion. The 1 μm thin sections were stable enough to perform AFM characterization without material coalescence. These thin sections could also be characterized using light microscopy under normal transmitted light and phase-contrast imaging modes prior to AFM characterization.

Asphaltenes, SBS, and MDI model molecules are studied in this paper (**Figure 1**). The three asphaltene molecules (denoted as AS1, AS2, and AS3 in **Figure 1a, b, c**) are those suggested by Martin-Martinez et al. as most stable isomers from the Mullins-Yen model based on Clar Sextet Theory.[20,21] Given the challenges with the detailed characterization of the asphaltenes, it is commonly accepted to use a limited number of structures to describe the average asphaltenes in asphalt. Thus, we have built on previous work from Greenfield et al.,[15–17] Mullins et al.,[18,20] and Martin-Martinez et al.,[21] to select the asphaltene molecules used in this study. Because SBS is a block copolymer, the individual styrene and butadiene components were considered separated for the calculations, thus isolating the interactions of each functional group individually. To make the computations more tractable, a smaller system of a dimer of polystyrene (denoted as S in **Figure 1d**) and a dimer of polybutadiene (denoted as B in **Figure 1e**) were selected. In the case of MDI, three structures are considered, namely, monomeric MDI (denoted as M), polymeric MDI (denoted as M_P) and two reacted forms of MDI. These reacted forms are: MDI reacted with water (denoted as M_{R_H2O}) according to Equation 1 to yield a urea linkage, and MDI reacted with the hydroxy group of AS2 (denoted as M_{R_AS2}) to form a urethane linkage, following Equation 2.[6] We are aware that MDI reacts in the presence of a polyol to form a polyurethane, but because this functional group is already included in the selected model molecules for this study, the MDI-polyol reaction is not included explicitly here.

$$R^1 - NCO + H_2O \rightarrow R^1 - NH_2 + CO_2 \quad (1a)$$

$$R^2 - NCO + R^1 - NH_2 \rightarrow R^2 - NH - CO - NH - R^1 \quad (1b)$$

$$R^1 - NCO + R^2 - OH \rightarrow R^1 - NH - COO - R^2 \quad (2)$$

To evaluate the effect of π–π stacking and intermolecular interactions in the clustering of asphaltenes, stacked arrangements of SBS, MDI and asphaltene model systems are used. According to the well-accepted Mullins-Yen model for asphalt, asphaltene molecules normally arrange in clusters due to π–π interaction between the aromatic cores.[20] In our case the stacked asphaltene molecular systems are referred to in **Figure 1i** by the numbers of the asphaltenes constituting them, e.g. “33” for and AS3-AS3 stack, or as “AS stacks” when referring to the set of all the three possible stacks, i.e., “11”,”22”,”33” stacks at once.

Furthermore, we consider two scenarios of additives interacting with asphaltene molecules. In the sandwich arrangement, additives are added to the top and bottom of the asphaltene stack, in order to evaluate how the different additives affect the stacking distance and electronic structure of asphaltenes. The sandwich stack geometry, as shown in **Figure 1j**, is referred to by the first letter of the additive and the number of the asphaltene stack, as described above (e.g. “B11B” for butadiene–11 stack–butadiene, or “M11M” for MDI–11 stack–MDI). In the intercalated arrangement, additives directly interfere with the π–π stacking geometry of asphaltenes, by placing them in between asphaltene molecules. In fact, we arrange the additives to intercalate within the asphaltene stacks following recent studies that suggest that asphaltene aliphatic tails can interfere with π–π stacking in a similar fashion.[31] SBS-asphaltene stacks were used as a

comparison for the interaction of asphaltenes with MDI. This intercalated stack geometry, as shown in **Figure 1k**, is referred to by the number of the asphaltene and the first letter of the additive (e.g. "1M1", for a AS1–MDI–AS1 system). Not all the intercalated molecular systems we considered converged to stable structures, therefore only geometries for which additives are stably intercalated into the asphaltene stack are included for analysis.

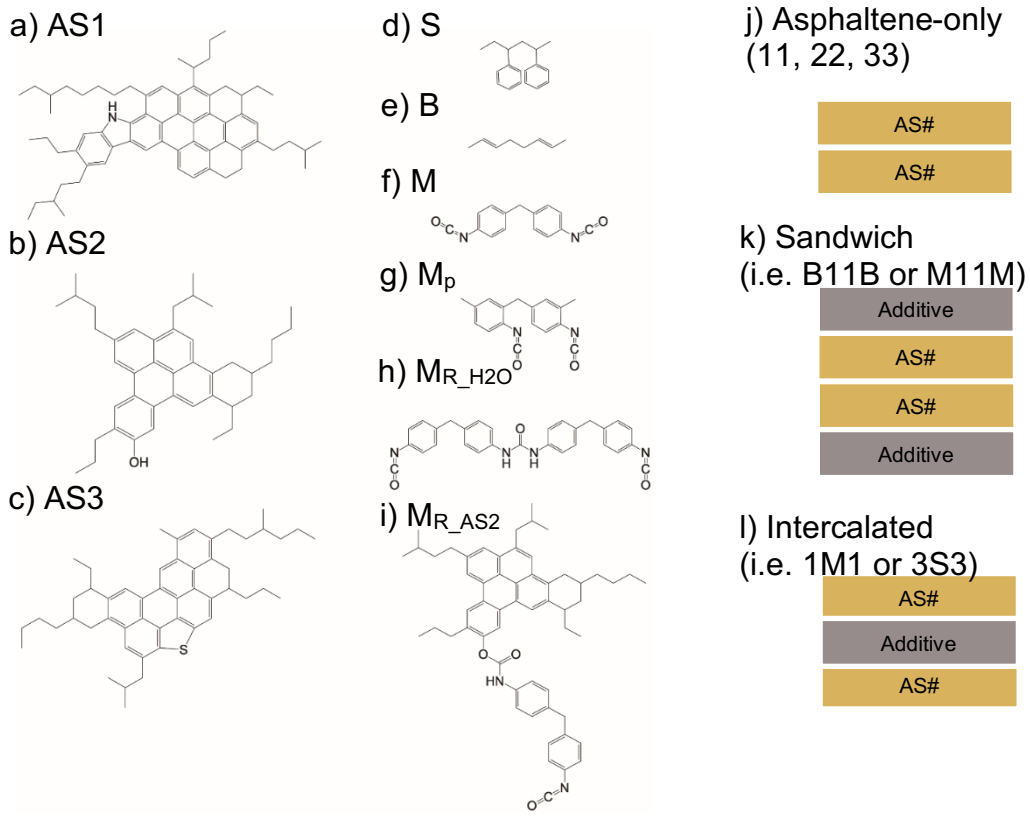

Figure 1. Model molecules studied in this work. Asphaltene molecules from [21] a) AS1, b) AS2, c) AS3. Additives included SBS rubber, which were divided into small molecules of d) styrene (STY) and e) butadiene (BUT). MDI studied includes f) monomeric form (M), g) polymeric form as a dimer (M_P), h) MDI reacted with water (M_{R_H2O}), and i) MDI reacted via the –OH group of AS2 (M_{R_AS2}). Example of stacked configurations with j) two pi-pi stacked asphaltene molecules, k) sandwich stack with additive-asphalt-asphalt-additive, and l) intercalated stack.

All molecules under study are optimized with a semi-empirical tight-binding method xtB-GFN2 CREST,[32–35] which is specially parametrized for geometries, frequencies, and noncovalent interactions. CREST applies a metadynamics bias potential to efficiently explore the conformational and energy landscape of molecules, enabling rapid identification of minimum energy geometries. This metadynamics method is more likely to prevent the molecules from becoming trapped in a local minimum. The CREST-optimized geometries are further refined with DFT calculations using the ORCA package to more accurately compute the singlet ground state energies. The PBEh-3c functional,[33] which is optimized to properly describe noncovalent interactions, is used in conjunction with the 6-31G* basis set.[36,37] This split-valence double-zeta basis set has been already used in modeling asphaltene compounds.[21,38–40] A geometrical counterpoise correction (gCP) is applied to correct for basis set superposition error.[33] The same DFT method is used to calculate the polarizability, chemical softness, and frontier orbitals of the molecular stacks. CREST was also used in conjunction with the GFN force field to calculate

geometries and mixing energies for oligomers without subsequent DFT refinement. This force field is to an extent polarizable and treats dispersion interactions with a simplified version of the established D4 scheme that is the most recent version of Grimme dispersion.

Reaction rate calculations were performed on the BASF supercomputer using Turbomole version 7.5 and COSMOTherm version 19 with parameterization BP-TZVPD-FINE 2018. Conformational searches and structure optimizations were done using the tpssh exchange-correlation functional with a def2-TZVP basis set, D3 dispersion correction and COSMO solvation with a dielectric constant of 2.4. Final single-point energies were calculated using M06-2X with the def2-QZVP basis with equivalent COSMO settings and without dispersion corrections. Free energies were determined with contributions from vibration (RRHO), rotation and translation (ideal gas), as well as COSMO-RS solvation using ethylbenzene as the effective medium. Ethylbenzene was chosen as medium because it contains 75% aromatic and 25% aliphatic carbons. Kinetic rate constants were calculated using classical transition state theory. An approximate tunneling correction to the rate constant was applied.[41]

Binding energies, π–π stacking distance, chemical softness, polarizability, and kinetic rate constants are calculated.

The π–π stacking exhibited between the aromatic cores of asphaltenes is thought to be the primary contribution to the formation of clusters in asphalt.[24] The morphology of these clusters is indicative of phase separation in polymer-modified asphalt, i.e., larger π–π stacking distance indicates weaker π–π interactions and lower clustering, which improves phase continuity.[20] In the study of polycyclic aromatic hydrocarbons (PAHs), the π–π stacking distance is generally calculated as the z-distance between centers of mass of the polycyclic aromatic cores, with ~3.8 Å denoting the π–π stacking cutoff distance. In order to determine the vertical distance between asphaltene center of masses, the perpendicular distances between asphaltene centers of mass were averaged to give the final π–π stacking distance of the slightly misaligned stacks.

To better quantify the effects of additives on asphaltene stacks, the binding energy is quantified according to Equation 3 and Equation 4. The binding energy is calculated by subtracting the energy of the single component clusters from the mixed clusters.

Sandwich stack: $E_{binding} = E_{calculated} - (E_{MDI\text{-}MDI} + E_{Asphaltene\text{-}Asphaltene})$ (3)

Intercalated stack: $E_{binding} = E_{calculated} - (½\ E_{MDI\text{-}MDI} + E_{Asphaltene\text{-}Asphaltene})$ (4)

Chemical softness and polarizability are also computed as indicators of the molecules to engage in chemical reactions.[42,43] Chemical softness is the inverse of the chemical hardness, which is resistance of the chemical potential to change in the number of electrons.[44] Chemical hardness is commonly defined as the second derivative of the electronic energy with respect to the number of electrons or simply estimated as ionization potential (IP) minus electron affinity (EA).[45–47] In this paper, the chemical softness is calculated as 1/(IP - EA). The values of IP and EA are estimated according to Koopman's Theorem, which states that the first ionization energy can be approximated by the negative of the HOMO energy, while the electron affinity is approximated by the negative of the LUMO energy.[48] Following the suggestion of Tozer et al.,[46] Equation 5 and Equation 6 are used to calculate IP and EA. This method is expected to mitigate the error

arising from the Koopman's Theorem approximation. The chemical softness and polarizability are known to increase with the size of the molecule, and therefore normalizing the data helps to visualize the effects of the additives decoupled from the effects of the size of the molecular arrangements. Therefore, the linear trend between chemical softness, cube root of polarizability, and number of atoms was used to normalize the data, following available literature.[49]

$IP = (E_{N-1}) - E_N$ N = number of electrons in neutral molecule (5)

$EA = -(E_{LUMO} + E_{HOMO}) - IP$ (6)

Polarizability is a measure of how easily the electron density of a molecule is deformed in response to an external electric field from other molecules such as ions or dipoles.[50] A lower chemical softness is generally correlated with a lower polarizability and lower reactivity.

Kinetic rate constants are also computed to determine the likelihood of chemical reactions between different components of the asphalt mix. These constants indicate the likelihood of reaction between relevant species.

Results and Discussion

Rheological characterization

		Top	Bottom	% diff
Control	G*sin d (kPa)	1.201	1.264	4.98
	Phase (degrees)	87.42	87.4	
SBS	G*sin d (kPa)	2.665	2.611	2.01
	Phase (degrees)	74.3	74.4	
Reactive isocyanate	G*sin d (kPa)	3.496	3.387	3.12
	Phase (degrees)	80.7	81	
SBS+Reactive isocyanate	G*sin d (kPa)	5.792	5.718	1.27
	Phase (degrees)	67.7	67.8	

Table 1. DSR of asphalt blends for dynamic and phase angle properties. The control asphalt-only, SBS, commercial reactive isocyanate, and SBS-reactive isocyanate asphalt blends all demonstrate excellent mechanical stability in this separation test at 64ºC. Reactive isocyanate modified SBS-asphalt has the smallest difference in phase separation between the top and bottom samples of this test.

To characterize the tendency of the additives to separate from additive-modified asphalt under static heated storage conditions, separation testing with the DSR was used. **Table 1** demonstrates the measured values for the stability of the various blends. Altogether, all four blends (asphalt-only, SBS-modified, reactive isocyanate-modified, and SBS- reactive isocyanate-modified) are stable with minimal differences in test results between top and bottom specimen. When combined with reactive isocyanates, SBS-modified asphalt demonstrates the least percent difference between properties of the top and bottom specimens, indicating a smaller degree of incompatibility between the polymer and base asphalt. These encouraging results indicate that

reactive isocyanates do not negatively affect the mechanical stability of SBS-modified asphalt and that very little of the polymer additives separate from the asphalt during testing.

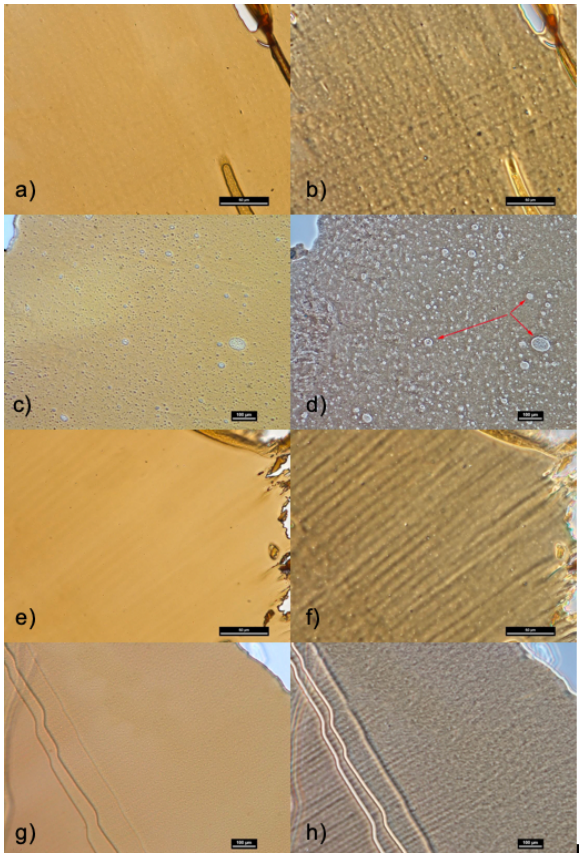

Figure 2. Microstructures of asphalt blends by light microscopy. 1µm thin sections viewed at 400x magnification using transmitted light (left column) and phase-contrast (right column) for asphalt-only (a, b) asphalt-SBS (c, d), asphalt-reactive isocyanate (e, f) and asphalt-2% SBS-2% reactive isocyanate (g, h). Asphalt-SBS (c, d) have clear microstructural phase separation through the formation of observable rubber particles. When reactive isocyanates are added to SBS-modified (g, h), the phase separation is no longer visible, and the modified asphalt mixture looks similar to the asphalt-only microstructure.

Structural characterization

Light microscopy and AFM studies allowed further characterization of the microstructures of additive-modified asphalt to better understand the role of isocyanates in affecting the stability of asphalt. Asphalt-only samples have microscopic domains dispersed uniformly throughout the sample that are invisible under normal, transmitted light (**Figure 2a)** but visible under phase-contrast illumination **(Figure 2b)**. Note that this is not inconsistent with other asphaltene studies where asphaltene clusters are observed in bulk samples in crude oils and toluenes. This sample is a thin 1 um cross section and there is likely not enough wax exudation to observe the nanoaggregates as a result. This sample was used as a control to compare to the other asphalt blends. When SBS is added to asphalt, rubber particles with spherical domains of 10-100 µm diameter are visible and dispersed uniformly throughout the sample (**Figure 2c, d)**. The presence of these particles indicates that SBS exhibits microstructural phase separation from asphalt. In contrast, when isocyanates are added, there is no evidence of isocyanate particles visible in the phase-contrast image (**Figure 2e, f**) and the asphalt-isocyanate sample looks like the asphalt-only sample. When the reactive isocyanate from BASF is added to SBS-modified asphalt, the rubber particles are significantly less visible (**Figure 2g, h)**. These results indicate that adding reactive isocyanates to SBS-modified asphalt helps eliminate visible particles and prevent microphase separation in the form of microstructures within the asphalt blend. This suggests that isocyanates play a large role in structurally stabilizing SBS-modified asphalt, likely acting as a compatibilizer between asphaltenes and SBS.

To verify, TappingMode™ AFM was performed on the 1µm thin sections (on mica). **Figure 3** shows height (topography) and phase (viscoelasticity) images of the asphalt-only (**Figure 3a, b**), asphalt+SBS (**Figure 3c, d**), and asphalt+SBS+commercial reactive isocyanates from BASF

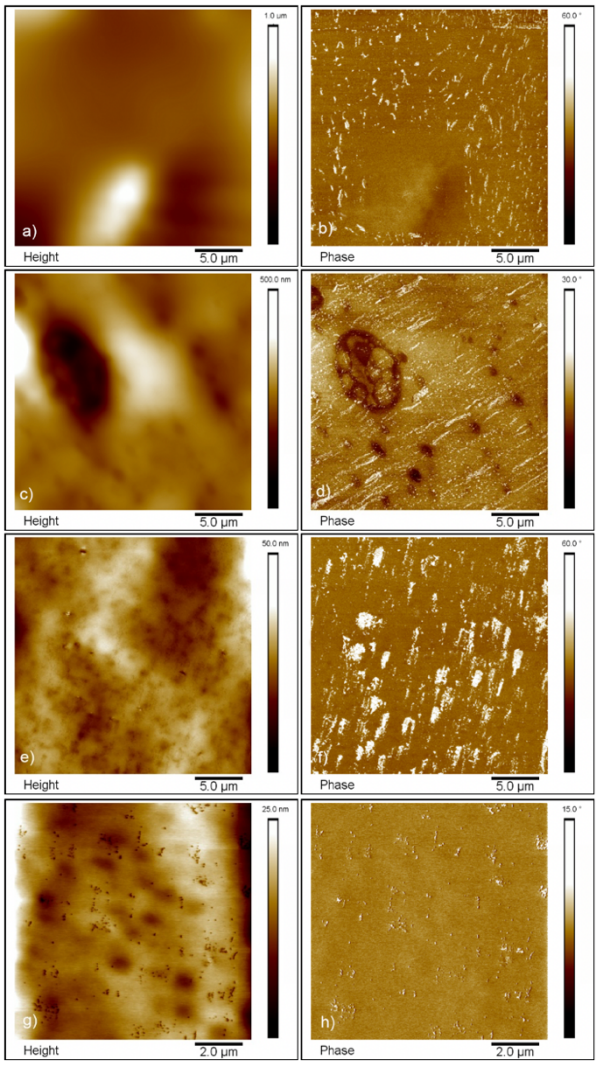

Figure 3. TappingMode™ AFM Height (left) and Phase (right) images of 1µm thin sections at 25µm x 25µm scan areas for asphalt-only (a, b), asphalt-SBS (c, d), and asphalt-2% SBS-2% reactive isocyanate (e, f) and a 10µm x 10µm scan area for asphalt-2% SBS-2% reactive isocyanate (g, h). Asphalt-SBS (c, d) have clear microstructural phase separation through the formation of observable rubber particles that appear as shallow depressions in the height images and distinct, softer/darker domains in the phase images. When reactive isocyanates are added to SBS-modified asphalt (g, h), the phase separation is no longer visible, and the modified asphalt mixture looks similar to the asphalt-only microstructure with the exception of small, shallow depressions in the height images that are suspected rubber domains reduced in size and require higher magnification to observe (g, h). Bright domains in phase images of all samples are presumed wax in the asphaltene core.

(**Figure 3e-h**) samples. AFM phase imaging of the asphalt-only sample showed only microscopic surface domains presumed to be wax exudation. Addition of SBS rubber showed discrete domains consisting of depressions in the height images and darker/softer contrasting domains in the phase images. These domains disappeared in the reactive-isocyanate-modified asphalt+SBS sample (e, f). However, smaller, shallower depressions were observed in the height images that may be rubber domains reduced in size by the addition of the reactive isocyanates (g, h). Lack of contrast between the rubber and asphalt matrix in the phase images suggest that the reactive isocyanates render the rubber domains more soluble and miscible in the asphalt, leading to smaller, more numerous domain sizes that are not detectable by AFM under the current imaging conditions.

π–π stacking, binding energy, and noncovalent interactions between asphaltene aromatic cores in sandwich stacks

To determine whether π–π stacking interactions may be contributing to the observed stabilization of reactive-isocyanate-modified asphalt, we quantified the π–π stacking between molecules by measuring the distance between the center of mass of the polycyclic aromatic core of the asphaltenes. **Table 2** shows the values for the π–π stacking distances of all sandwich stacks. It can be seen that the differences in π–π stacking distances from the initial AS stacks, without additives, are less than 0.2 Å when additives are included. This indicates an almost negligible effect on the π–π stacking distances from additives surrounding a stacked asphaltenes aromatic core, likely because of the already strong π–π interactions

Molecule	AS1	AS2	AS3
AS stack	3.722	3.602	3.656
S	3.648	3.476	3.806
B	3.817	3.400	3.668
M	3.563	3.504	3.504
M_P	3.570	3.543	3.645
M_{R_H2O}	3.644	3.573	3.606
M_{R_AS2}	-	3.534	-

Table 2. π−π stacking distance (Å) for sandwich stacks. The rows indicate the additive and the columns indicate the asphaltene with which they were stacked. No pi-pi stacking distance is computed for M_{R_AS2} with AS1 or AS3 because M_R is reacted with AS2 as discussed in section 2. There is π−π interaction between the asphaltene molecules in all the sandwich stacks. Additives in the stacking arrangements do not significantly affect π−π stacking distance between the center of mass of the polycyclic aromatic core of the asphaltenes.

This also indicates that a π−π stacking geometrical arrangement alone is unlikely to explain the stabilization observed from the addition of MDI to the asphalt blend. A reduction of asphaltene clustering, by the effect of MDI into the π−π stacking distances is not observed. Therefore, we expect electronic effects, and other noncovalent interactions to contribute to MDI's stabilization on SBS – asphaltene systems. This is further confirmed by analyzing the aromaticity of the polycyclic aromatic core of the asphaltenes in the sandwich stacks from the initial asphaltene-only arrangement. To this end we calculated the mean bond dispersion (MBD) and the mean bond length (MBL) of the aromatic rings in the asphaltenes,[51–53] which has been shown to accurately describe aromaticity changes in polycyclic aromatic systems like carbon nanotubes and graphene nanoribbons. No significant changes in the aromaticity were observed. Since the MBD and MBL did not show any relevant information, we do not include the images here. The results indicate that aromaticity of the asphaltene polycyclic aromatic cores is preserved after the addition of the additives in a sandwich stack.

Unsurprisingly, the intercalated stacks disrupt the π−π stacking of asphaltene polycyclic aromatic cores resulting in a separation distance of larger than 3.8 Å (not included in the table), which is too far apart for π−π stacking to be considered.

We next examine MDI, the key molecular component of the reactive isocyanates-modified asphalt. To evaluate whether MDI interactions with asphaltenes are favorable, several energies were computed in **Table 3** for the intercalated and sandwich stacks. Specifically, binding energy, as explained in section 2.4.1, was used to quantify the additional favorable MDI interaction contributes the asphaltene stacks. We note that though all combinations of asphaltene and additives were tested in intercalated stack geometries, only the stacks where additives remained intercalated after CREST metadynamics optimization are shown: monomeric MDI (M), polymeric MDI (M_P), and water reacted MDI (M_{R_H2O}).

Molecule	AS1		AS2		AS3	
AS stack	-1.266		-0.861		-1.065	
S	0.1277	—	-0.0036	—	0.4924	—

B	-0.2002	—	-0.2551	—	-0.1838	—
M	-0.2587	-0.1453	-0.2522	—	-0.1694	0.0439
M_P	-0.4408	—	-0.0832	—	-0.1007	0.1229
M_{R_H2O}	-0.1505	-0.1387	-0.5852	-0.2783	-0.0314	0.0785

Table 3. Binding energy (eV) of additive-asphaltene sandwich stack or intercalated stack. The rows indicate the additive and the columns indicate the asphaltene with which they were stacked. Light grey indicates the intercalated stack (i.e. 1M1). Binding energies are computed according to Equation 3 for the sandwich stacks and Equation 4 for the intercalated stacks. Most sandwich stacks have a slightly negative, favorable binding energy. The intercalated stacks are always less favorable than the sandwich stacks. MDI additives are generally more stable than styrene additives stacked with asphaltene molecules. Further, MDI is the only additive that can stably intercalate with asphaltene molecules.

Most sandwich stacks and remaining intercalated stacks have negative, favorable binding energies, indicating that the additives contribute additional physical interactions to the asphaltene molecules that help stabilize the sandwich and intercalated stacks (**Table 3**). The interaction energy value for sandwich stacks is more negative than for their corresponding intercalated stacks, because the aromatic pi-pi stacking interactions of the asphaltene cores are preserved in the sandwich arrangement. MDI additives on both sandwich and intercalated stacks exhibited a lower binding energy, or stronger binding strength that styrene additives for most of the stacks. This is likely due to the inability of the phenyl group of polystyrene, to experience π interactions with the aromatic asphaltene core. This is in line with that fact that polystyrene has only been found to form intrachain π–π stacking in specific appropriate environments such as more crystalline, syndiotactic polymers or conditions which favor rotational isomers.[54–57] Interestingly, butadiene has similar binding energies to asphaltenes as MDI with asphaltenes suggesting that MDI would interact with the butadiene domains of SBS more strongly with the styrene domains.

To better understand how different additives affect the stacking of asphaltene molecules, and also with the aim to characterize the nature of the intermolecular interactions, we perform a frontiers orbital analysis in the different stacks under study. Thus, we calculated the highest occupied molecular orbital (HOMO) and lowest unoccupied molecular orbital (LUMO), which were then visualized for all additive-AS1 clusters in both sandwich and intercalated forms (**Figure 4**). In the 11 stack (**Figure 4a**), HOMO and LUMO are localized on the asphaltene cores. In contrast, 11 stacked with the different additives exhibits HOMO localized on both asphaltene cores, but LUMO localized often on only one asphaltene. This indicates that all additive stacks experience interactions with asphaltene molecules that are not solely electrostatic.

The lack of an aromatic core in butadiene hampers its π–π stacking with asphaltenes, as can be seen in the B11B sandwich arrangement in **Figure 4b**. However, even though styrene has an aromatic phenyl group, it does not stack with AS1 via π–π interactions, and no alignment of aromatic rings is observed between the two molecules (**Figure 4c**).

In contrast, MDI clearly exhibits noncovalent π–π interactions with AS1 and has a stabilizing electronic structure when stacked with asphaltene molecules (**Figure 4d-f**). This stronger interaction is observed in the alignment of the polycyclic aromatic core of the asphaltene and the aromatic rings of MDI, and the localization of HOMO and LUMO on both molecules of the

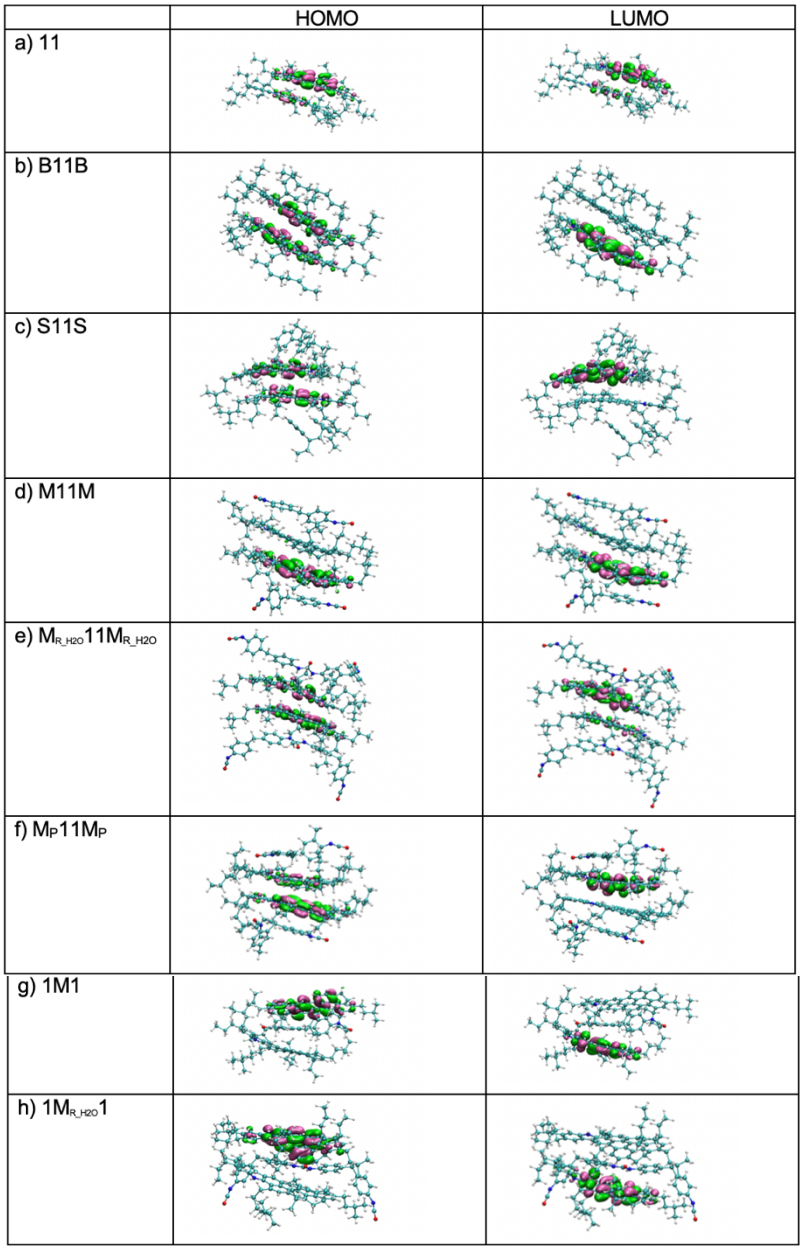

Figure 4. Select HOMO and LUMO of optimized geometries of interest with AS1. (a-h) Plotted at an isosurface value of 0.03. MDI additives (d, e) have HOMO and LUMO on both asphaltene molecules, indicating a stabilized electronic structure. In contrast, other structures have HOMO and LUMO localized on only one molecule, indicating a more destabilized electronic interaction.

asphaltene core (**Figure 4d**). The orbital interaction in the π–π stacked structures is even more pronounced in the sandwich stack with the MDI_{R_H2O} (**Figure 4e**). This orbital interaction is expected to stabilize the cluster, and it is coherent with the higher binding strength for MDI – asphaltene compared to styrene or butadiene ones, as shown in **Table 2**.

The disruption of π–π stacking is present in the intercalated stacks, such as 1M1 (**Figure 4g**) and $1M_{R\_H2O}1$ (**Figure 4h**), where even though the additive is π–π stacked between the asphaltene molecules, HOMO and LUMO are localized only on one of the asphaltenes. This is consistent with the large π–π distance for intercalated stacks in Section 3.2. This break in symmetry between HOMO and LUMO indicates that the intercalation of additives destabilizes the complex. This indicates a weaker interaction, and it points out that the asphaltene – asphaltene stacking is essential to the stability. Therefore, a sandwich arrangement will be preferred. Longer MDI molecules are able to have more HOMO and LUMO interaction with the asphaltene molecules. $1M_{R\_H2O}1$ (**Figure 4h**) has more interaction because two phenyl rings are aligned with the asphaltene aromatic cores, compared to one phenyl ring in 1M1 (**Figure 4g**). The rigid urea conformation allows M_{R_H2O} to stay locked in this binding arrangement. This likely contributes to the greater stability and lower softness of M_{R_H2O} intercalated with asphaltenes discussed later (**Figure 5a**). This emphasizes the need to employ several MDI conformations (monomer, polymeric, reacted) in a model that aims to achieve an accurate description of MDI – asphaltene interactions.

From these simulations, the stabilization MDI confers on asphalt is remains unclear. While the binding energies between MDI and asphalt and SBS and asphalt shows minimal differences, frontier orbital analysis suggests that MDI may be contributing a degree of noncovalent π–π stacking interactions to the asphalt as compared to SBS which does not demonstrate this noncovalent interaction.

Noncovalent oligomeric effects

As shown in the frontier orbitals analysis, $1M_{R\_H2O}1$ has more interaction with the asphaltene than 1M1 because it is a larger molecule. To determine whether the phase stabilizing effect due to noncovalent interactions with MDI and SBS is more apparent in larger molecular systems, we next studied oligomers of PMDI and SBS. In order to calculate the favorability of MDI mixing with SBS, we used the general mixing energy equation:

$$E_{mix} = E_{AB} - \tfrac{1}{2}(E_{AA} + E_{BB}) \quad (7)$$

The use of this simple, and easily evaluated, mixing rule is supported by the fact that the entropy of mixing of a polymer blend is typically very nearly 0 or even slightly negative. This is particularly true for significant degrees of polymerization, as would certainly be the case for commercial SBS and oligomeric MDI. Therefore, the contribution of entropic effects to the free energy of mixing would be negligible or slightly positive. Therefore, the mixing energy (as estimated with equation 7), or enthalpy, would be the dominant contributor to the free energy.

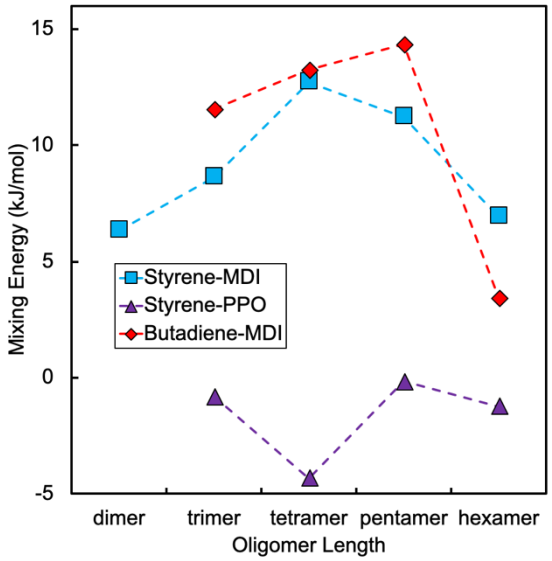

PMDI oligomers of lengths 2 to 6 were simulated with BUT and STY oligomers of similar physical length. As before, the PMDI dimers, additive dimers, and PMDI-additive pairs were optimized by CREST metadynamics and the GFN-FF force field to achieve the lowest energy configuration. Positive mixing energies were found for both oligomers of STY with PMDI, and BUT with PMDI. Interaction energy rises as oligomer length increases before dropping at the largest end of the studied oligomers (**Figure 5**). This is most likely due to the ability of longer oligomers to fold back on themselves, reducing the interaction between the oligomers of incompatible components. Furthermore, application of equation 7 to oligomers (from two to six monomeric units) of polyphenylene oxide (PPO) and polystyrene result in negative mixing energies within the currently employed methodology (results not reported). These two polymers are well known to form a compatible, single-phase blend with a single glass transition temperature.These results suggest that noncovalent interactions of PMDI with SBS oligomers cannot explain the phase stabilizing effect of PMDI in SBS modified asphalt.

3.4 Proposed MDI stabilization mechanisms of SBS-asphaltene from rate of reaction

The aforementioned series of calculations were undertaken to determine the degree to which noncovalent interactions play a role in the phase stability of polymer-modified (SBS) asphalt blends. Given the result of positive interaction energies between all the studied oligomers, we suggest that this mechanism may contribute only to a limited degree.

As a result of this finding, we have additionally investigated a potential mechanism which involves the reaction of isocyanate groups with two species; asphaltenes and other aromatics that contain polar groups with active hydrogen atoms (-OH, -NH, -COOH, etc.) and the unsaturation contained within the butadiene domains of SBS. As previously stated, the reaction of isocyanate with polar groups on asphaltene moieties in a polymer-modified asphalt blend has been reported in the literature.[7,58] In addition, the proposed cycloaddition reaction has also been reported to take place under mild conditions at room temperature,[59] and has been studied with *ab initio* calculations,[60,61] albeit with activated isocyanates, and has been used to prepare β-lactams, the key structural unit in penicillin-based antibiotics. Further, butadiene was considered because isocyanates can generally undergo cycloaddition reactions with other unsaturated functionalities such as the non-aromatic unsaturation of butadiene. In contrast, this reaction has not been previously reported in a polymer-modified asphalt blend.

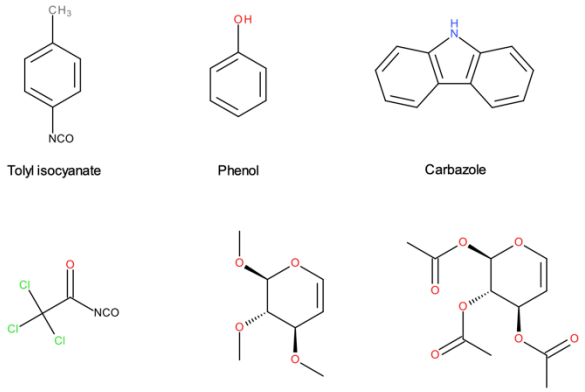

Figure 6. Chemical Structures of studied compounds for kinetic rate computations.

To test our hypothesis, we performed DFT calculations for reactants, transition states and products in the reaction of tolyl isocyanate with phenol, carbazole and cis-2-butene. The reactions with phenol and carbazole form a basis for comparison to the cycloaddition with butadiene. Tolyl isocyanate provides a model for 4,4'-MDI, while phenol and carbazole provide models of asphaltenes and aromatics with polar functionalities (**Figure 6**). Cis-2-butene was chosen as a model for the butadiene phase of SBS because the isocyanate approach to the double bond of this isomer is less hindered, and thus this isomer will manifest a higher rate constant for the reaction. The proportion of the cis isomer has been measured by NMR peak integration to be roughly 40 mole% [62] in a few commercial-grade SBS samples, as well as a commercial grade polybutadiene homopolymer. Furthermore, the reactions with phenol and carbazole were modeled as first order in -OH and -NH, that is the transition states were bi-molecular. The reactions were treated in this manner because of the limited concentration of asphaltene functional groups and high viscosity of the asphalt blend. We note that in solution, and at a high concentration of active hydrogen functional groups, the reaction is second order in -XH, which corresponds to a termolecular transition state.

The results of our calculations are presented in **Table 4**. The reactions are predicted to not take place at low temperature but do proceed at the mixing temperature of asphalt blends. With the

exception of the reaction with carbazole, the equilibrium constants for each reaction lie on the products side. Most importantly, the rate of reaction with cis-2-butene is calculated to be competitive with that of phenol. Given that the reaction with functionalized asphaltene has been reported in the literature, we suggest that a reaction with the butadiene phase of SBS may also take place. A reaction such as this, will form an in-situ, covalent "tie-layer" between phases that can compatibilize the phases and improve the properties of the asphalt blend. In other words, MDI can react with asphalt groups as well as the butadiene in SBS to form a covalent link between the two phases. Such a covalent link could be presumed to prevent phase separation, similar to the role sulfur plays in crosslinking and preventing phase separation of SBS-asphalt.[2]

Compound	$k_{forward}$ 30ºC	$k_{reverse}$ 30ºC	$k_{forward}$ 180ºC	$k_{reverse}$ 180ºC
Phenol	$<10^{-18}$	$<10^{-18}$	1.6×10^{-7}	3.6×10^{-8}
Carbazole	$<10^{-18}$	$<10^{-18}$	6.9×10^{-8}	1.1×10^{-6}
Cis-2-butene	7.6×10^{-15}	$<10^{-18}$	2.6×10^{-7}	9.5×10^{-8}

Table 4 – DFT Calculated Kinetic Rate Constants (l/mol/hr) for Reaction of Tolyl Isocyanate with Phenol, Carbazole and Cis-2-butene. Kinetic rate constants demonstrate that reactions do not take place at room temperature, but take place under elevated temperatures at which asphalt is processed. The rate of reaction of the tolyl isocyanate is similar to the phenol, indicating that butadiene reactions with isocyanate may help compatibilize the different phases.

As an estimate of the reliability and accuracy of our calculations for the cycloaddition, we have also included the experimental results of Grinstaff et al, on the activated trichloroacetyl isocyanate, in **Table 5** for comparison to the reaction with tolyl isocyanate. Here we have taken the reported coordinates of each glycal as starting point for our calculations. We can see that our calculated rates are roughly 2-3 orders of magnitude lower than the experimental results. This discrepancy can arise due to many factors, such as the choice of exchange-correlation functional, the basis set size, and the approximate treatment of solvation. Furthermore, the exponential dependence of the rate constant on the activation free energy imposes a stringent requirement for the calculation of absolute rate constants, i.e., a slight error in activation free energy gives rise to a large difference in rate constant. Most importantly, while the absolute rate constants do not agree with experiment, the trend in relative rates are well reproduced. Given the similarity between the cycloaddition reactions of the glycals and cis-2-butene and assuming a systematic error, we suggest that the reaction rate constant of an isocyanate and the unsaturation present in SBS may be even greater. We should also note that our own previously unreported calculations of the kinetic rate constants for the urethanization reaction of phenyl isocyanate and aliphatic alcohols, using the same methodology, deviate by less than one order of magnitude from the available experimental results. This lends further credence to the calculations for phenol and carbazole. Assuming a systematic error, this suggests that the proposed reactions within asphalt may be even more feasible.

Compound	DFT	Experimental

Glycal A	**2.5×10^{-5}**	**4.5×10^{-3}**
Glycal B	**1.6×10^{-8}**	**5.5×10^{-5}**

Table 5 – DFT Calculated (at 30C) and Experimental Kinetic Rate Constants (at room temperature) (l/mol/sec) for Reaction of Trichloroacetyl Isocyanate with Protected Glycals. Our calculated rates are roughly 2-3 orders of magnitude lower than the experimental results, while the calculated relative rates are well reproduced providing a good test of the reliability and accuracy of our calculations for the cycloaddition suggested in Table 4. Assuming a systematic error, this suggests that the proposed reactions within asphalt may be even more feasible.

We should note that the high viscosities of the asphalt blends can certainly limit the reaction rates due to mass transfer limitations. Nonetheless, given the high reaction temperature, long reaction times and aggressive mixing of the components, we propose that the reactions can take place at a reasonable rate under the conditions imposed during sample preparation.

Potential aging properties

Reactions between isocyanates and SBS-modified asphalt may contribute to the observed decrease in phase separation discussed above. In addition to these enhanced phase stability properties of additive-asphaltene stacks, chemical reactivity parameters were also computed to determine the tendency of the asphaltene stacks to be affected by oxidative agents. Although it is difficult to fully account for the various chemical reactions that occur during oxidation, chemical reactivity parameters may describe how likely certain chemicals are to be oxidized and these parameters have been shown to corroborate experimental data of biomodified asphalt binders.[43]

Additives in the sandwich structure generally contribute to the lower chemical softness, and therefore lower reactivity and lower tendency of asphaltene molecules to be affected by oxidative agents. **Figure 7** shows the normalized data for chemical softness and polarizability calculations. Stacks that deviate significantly from the trendline are labeled in the chemical softness and cube root of polarizability graph.

Additives combined with AS1 stacks have consistent chemical softness values closer to those of the 11 stack, whereas additives with AS2 and AS3 have greater variance in their chemical softness values. For nearly all of the stacks except with AS3, the addition of chemical additives results in a lower chemical softness value and therefore lower reactivity. Notably, stacks with M_{R_H2O} and M_P have significantly low softness values given the size of the complex. As observed for binding energies above as well, this is likely due to the additional stabilizing benefit offered by more MDI additive groups present in these molecules that help avoid oxidation.

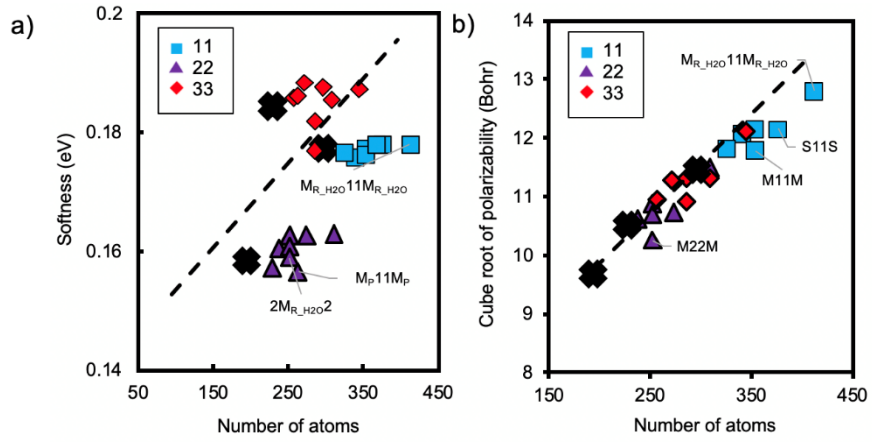

Figure 7. Normalized chemical reactivity descriptors (a) chemical softness and (b) polarizability. Chemical softness and polarizability have been normalized to the size of the stacks according to relationships developed by Ghanty et al. [49] to better compare across different functionalities. Trendlines for chemical softness and polarizability are computed based on the three AS stacks without additives. Significant outliers (>10% for softness and >6.5% for polarizability) from the expected chemical softness and polarizability trendlines are labeled. 11, 22, and 33 stacks are labeled with the black X markers.

Polarizability shows a more consistent trend where MDI and styrene additives with asphaltenes result in lower polarizability. From this data, it can be deduced that MDI and styrene additives contribute additional noncovalent interactions that help stabilize the asphaltene molecules and thereby result in lower polarizability, lower reactivity of the cluster, and therefore lower tendency towards oxidative agents in aging. Further experimental studies on MDI-modified asphalt would likely reveal these benefits.

Conclusion

In this paper, the role of MDI in stabilizing SBS-modified asphalt blends is discussed. Dynamic shear rheology and atomic force microscopy experiments are performed to characterize the mechanical stability and microstructure of asphalt blends. Semi-empirical tight binding with metadynamics and DFT calculations are performed to provide understanding of the effects that MDI and SBS additives have on the phase stability and mechanical properties of asphalt formulations.

First, our experiments suggest that MDI-modified (with commercial reactive isocyanates from BASF) SBS-asphalt exhibits less microstructural phase separation while maintaining macroscopic mechanical stability. Second, our simulations suggest that MDI-based additives can act as compatibilizing agents between SBS and asphaltene components of asphalt formulations. We determined this by evaluating multiple mechanisms to explain this compatibilization. From examining the electronic structure of additives stacked with asphaltenes, it was observed that MDI $\pi-\pi$ stacks with asphaltenes while butadiene and styrene do not. This orbital interaction

was initially expected to stabilize the MDI-asphaltene structure. However, the small difference between π–π stack distances of asphaltene cores in the presence of MDI, butadiene, and styrene suggests that noncovalent π–π stacks contribute only minimally to the enhanced phase stability of SBS in asphalt when MDI is added. Instead, this compatibilizing effect is likely the result of interactions of mostly covalent nature, through reactions between individual components. Our rate of reaction study supports the reaction of isocyanate with aromatics containing polar groups at the elevated mixing temperature of asphalt blends, which has already been studied and reported to take place. Most importantly, the rate of reaction study also supports the reaction of isocyanate with butadiene at the same elevated temperature, as hypothesized due to the ability for isocyanates to undergo cycloaddition reaction with the "unsaturation" in butadiene. The reaction of MDI with both aromatics and butadiene is a plausible mechanism for the role of MDI as a linkage between asphaltene and SBS phases in asphalt. Last, we also presented how MDI contributed to the lower chemical softness and polarizability of asphaltene stacks, indicating potential resistance to oxidative agents during aging of the material.

Further studies are required to more thoroughly understand how MDI interacts with asphalt. There are also additional interactions to be considered, such as T-shaped (σ–σ) or offset π-stacked (π–σ) geometries.[63] Increasing computational resources, will also allow larger networks of SBS rubber, MDI polymer, and asphaltenes to be simulated, and compared to the model systems studied here. For example, a coarse-grained study with appropriate interaction potentials of oligomers with reacted and unreacted asphaltenes could be analyzed to determine phase behavior of the formulation. These directions should be further explored. In any case, this work reveals that different forms of MDI (monomeric, polymeric, reacted) should be considered in further computational and experimental studies.

Funding Sources. This work was supported by BASF. E.K. would like to thank the NSF Graduate Research Fellowship. J.H.T would like to thank the MIT UROP office. Additional support was provided by ONR (N000141612333 and N000141912375).

References

(1) Pamplona, T. F.; De C. Amoni, B.; De Alencar, A. E. V.; Lima, A. P. D.; Ricardo, N. M. P. S.; Soares, J. B.; De A. Soares, S. Asphalt Binders Modified by SBS and SBS/Nanoclays: Effect on Rheological Properties. *J. Braz. Chem. Soc.* **2012**, *23* (4), 639–647. https://doi.org/10.1590/s0103-50532012000400008.

(2) Singh, S. K.; Kumar, Y.; Ravindranath, S. S. Thermal Degradation of SBS in Bitumen during Storage: Influence of Temperature, SBS Concentration, Polymer Type and Base Bitumen. *Polym. Degrad. Stab.* **2018**, *147* (October 2017), 64–75. https://doi.org/10.1016/j.polymdegradstab.2017.11.008.

(3) Wen, G.; Zhang, Y.; Zhang, Y.; Sun, K.; Fan, Y. Rheological Characterization of Storage-Stable SBS-Modified Asphalts. *Polymer Testing*. 2002, pp 295–302. https://doi.org/10.1016/S0142-9418(01)00086-1.

(4) Hou, Y.; Sun, W.; Das, P.; Song, X.; Wang, L.; Ge, Z.; Huang, Y. Coupled Navier–Stokes Phase-Field Model to Evaluate the Microscopic Phase Separation in Asphalt Binder under Thermal Loading. *J. Mater. Civ. Eng.* **2016**, *28* (10), 04016100. https://doi.org/10.1061/(asce)mt.1943-5533.0001581.

(5) Polacco, G.; Stastna, J.; Biondi, D.; Antonelli, F.; Vlachovicova, Z.; Zanzotto, L. Rheology of Asphalts Modified with Glycidylmethacrylate Functionalized Polymers. *J. Colloid Interface Sci.* **2004**, *280* (2), 366–373. https://doi.org/10.1016/j.jcis.2004.08.043.

(6) Xu, J.; Xia, T.; Yin, B.; Yang, M. Effect of MDI on the Structure and Properties of SBS Modified Bitumen. *Constr. Build. Mater.* **2020**, *250*, 118911. https://doi.org/10.1016/j.conbuildmat.2020.118911.

(7) Navarro, F. J.; Partal, P.; García-Morales, M.; Martinez-Boza, F. J.; Gallegos, C. Bitumen Modification with a Low-Molecular-Weight Reactive Isocyanate-Terminated Polymer. *Fuel* **2007**, *86* (15), 2291–2299. https://doi.org/10.1016/j.fuel.2007.01.023.

(8) Cong, L.; Yang, F.; Guo, G.; Ren, M.; Shi, J.; Tan, L. The Use of Polyurethane for Asphalt Pavement Engineering Applications: A State-of-the-Art Review. *Constr. Build. Mater.* **2019**, *225*, 1012–1025. https://doi.org/10.1016/j.conbuildmat.2019.07.213.

(9) Carrera, V.; Partal, P.; García-Morales, M.; Gallegos, C.; Pérez-Lepe, A. Effect of Processing on the Rheological Properties of Poly-Urethane/Urea Bituminous Products. *Fuel Process. Technol.* **2010**, *91* (9), 1139–1145. https://doi.org/10.1016/j.fuproc.2010.03.028.

(10) Lu, X.; Sjövall, P.; Soenen, H. Structural and Chemical Analysis of Bitumen Using Time-of-Flight Secondary Ion Mass Spectrometry (TOF-SIMS). *Fuel* **2017**, *199*, 206–218. https://doi.org/10.1016/j.fuel.2017.02.090.

(11) Corbett, L. W. Composition of Asphalt Based on Generic Fractionation, Using Solvent Deasphaltening, Elution-Adsorption Chromatography, and Densimetric Characterization.

Anal. Chem. **1969**, *41* (4), 576–579. https://doi.org/10.1021/ac60273a004.

(12) Artok, L.; Su, Y.; Hirose, Y.; Hosokawa, M.; Murata, S.; Nomura, M. Structure and Reactivity of Petroleum-Derived Asphaltene. *Energy and Fuels* **1999**, *13* (2), 287–296. https://doi.org/10.1021/ef980216a.

(13) Kowalewski, I.; Vandenbroucke, M.; Huc, A. Y.; Taylor, M. J.; Faulon, J. L. Preliminary Results on Molecular Modeling of Asphaltenes Using Structure Elucidation Programs in Conjunction with Molecular Simulation Programs. *Energy and Fuels* **1996**, *10* (1), 97–107. https://doi.org/10.1021/ef950106t.

(14) Groenzin, H.; Mullins, O. C. Molecular Size and Structure of Asphaltenes from Various Sources. *Energy and Fuels* **2000**, *14* (3), 677–684. https://doi.org/10.1021/ef990225z.

(15) Zhang, L.; Greenfield, M. L. Molecular Orientation in Model Asphalts Using Molecular Simulation. *Energy and Fuels* **2007**, *21* (2), 1102–1111. https://doi.org/10.1021/ef060449z.

(16) Li, D. D.; Greenfield, M. L. High Internal Energies of Proposed Asphaltene Structures. *Energy and Fuels* **2011**, *25* (8), 3698–3705. https://doi.org/10.1021/ef200507c.

(17) Li, D. D.; Greenfield, M. L. Chemical Compositions of Improved Model Asphalt Systems for Molecular Simulations. *Fuel* **2014**, *115*, 347–356. https://doi.org/10.1016/j.fuel.2013.07.012.

(18) Mullins, O. C.; Sabbah, H.; Eyssautier, J.; Pomerantz, A. E.; Barré, L.; Andrews, A. B.; Ruiz-Morales, Y.; Mostowfi, F.; McFarlane, R.; Goual, L.; et al. Advances in Asphaltene Science and the Yen-Mullins Model. In *Energy and Fuels*; 2012; Vol. 26, pp 3986–4003. https://doi.org/10.1021/ef300185p.

(19) Dickie, J. P.; Yen, T. F. Macrostructures of the Asphaltic Fractions by Various Instrumental Methods. *Anal. Chem.* **1967**, *39* (14), 1847–1852. https://doi.org/10.1021/ac50157a057.

(20) Mullins, O. C. The Modified Yen Model. In *Energy and Fuels*; 2010; Vol. 24, pp 2179–2207. https://doi.org/10.1021/ef900975e.

(21) Martín-Martínez, F. J.; Fini, E. H.; Buehler, M. J. Molecular Asphaltene Models Based on Clar Sextet Theory. *RSC Adv.* **2015**, *5* (1), 753–759. https://doi.org/10.1039/c4ra05694a.

(22) Clar, E. *The Aromatic Sextet*; Wiley: New York, 1972.

(23) Ruiz-Morales, Y.; Mullins, O. C. Singlet-Triplet and Triplet-Triplet Transitions of Asphaltene PAHs by Molecular Orbital Calculations. *Energy and Fuels* **2013**, *27* (9), 5017–5028. https://doi.org/10.1021/ef400168a.

(24) Mullins, O. C.; Seifert, D. J.; Zuo, J. Y.; Zeybek, M. Clusters of Asphaltene Nanoaggregates Observed in Oilfield Reservoirs. In *Energy and Fuels*; 2013; Vol. 27, pp

1752–1761. https://doi.org/10.1021/ef301338q.

(25) Mullins, O. C. The Asphaltenes. *Annu. Rev. Anal. Chem.* **2011**, *4*, 393–418. https://doi.org/10.1146/annurev-anchem-061010-113849.

(26) BASF. *MDI Handbook*; 2013.

(27) Saunders, J. H.; Slocombe, R. J. The Chemistry of the Organic Isocyanates. *Chem. Rev. Rev.* **1948**, *43* (2), 203–318.

(28) Fleischel, O.; Otero Martinez, I.; Schatz, W.; Wiebelhaus, D.; Eling, B.; Scherzer, D.; Ferbitz, J.; Praw, M.; Malonson, B. L.; Taylor, R. . Asphalt Composition Comprising Thermosetting Reactive Compounds. WO 2018/228840 A1, 2018.

(29) Fleischel, O.; Praw, M.; Schatz, W.; Malonson, B. L.; Otero Martinez, I.; Wiebelhaus, D. Asphalt Composition Comprising Monomeric MDI as Thermosetting Reactive Compounds. WO 2020/126585 A1, 2020.

(30) Praw, M.; Schatz, W.; Kadrmas, A.; Kirk, W.; Andrew, J.; Otero Martinez, I.; Malonson, B.; Fleischel, O. Asphalt Composition Comprising a Mixture of an Isocyanate and a Polymer as Performance Additives. WO 2020/035403 A1, 2020.

(31) Simionesie, D. Investigation of Asphaltene Aggregation with Synthetic Model Compounds an Experimental and Computational Study, University of Birmingham, 2017.

(32) Grimme, S.; Antony, J.; Ehrlich, S.; Krieg, H. A Consistent and Accurate Ab Initio Parametrization of Density Functional Dispersion Correction (DFT-D) for the 94 Elements H-Pu. *J. Chem. Phys.* **2010**, *132* (15), 154104. https://doi.org/10.1063/1.3382344.

(33) Grimme, S.; Brandenburg, J. G.; Bannwarth, C.; Hansen, A. Consistent Structures and Interactions by Density Functional Theory with Small Atomic Orbital Basis Sets. *J. Chem. Phys.* **2015**, *143* (5), 180901. https://doi.org/10.1063/1.4927476.

(34) Grimme, S.; Ehrlich, S.; Goerigk, L. Effect of the Damping Function in Dispersion Corrected Density Functional Theory. *J. Comput. Chem.* **2011**, *32* (7), 1456–1465. https://doi.org/10.1002/jcc.21759.

(35) Kruse, H.; Grimme, S. A Geometrical Correction for the Inter- and Intra-Molecular Basis Set Superposition Error in Hartree-Fock and Density Functional Theory Calculations for Large Systems. *J. Chem. Phys.* **2012**, *136* (15), 154101. https://doi.org/10.1063/1.3700154.

(36) Ditchfield, R.; Hehre, W. J.; Pople, J. A. Self-Consistent Molecular-Orbital Methods. IX. An Extended Gaussian-Type Basis for Molecular-Orbital Studies of Organic Molecules. *J. Chem. Phys.* **1971**, *54* (2), 720–723. https://doi.org/10.1063/1.1674902.

(37) Hehre, W. J.; Ditchfield, K.; Pople, J. A. Self-Consistent Molecular Orbital Methods. XII.

Further Extensions of Gaussian-Type Basis Sets for Use in Molecular Orbital Studies of Organic Molecules. *J. Chem. Phys.* **1972**, *56* (5), 2257–2261. https://doi.org/10.1063/1.1677527.

(38) Coelho, R. R.; Hovell, I.; Rajagopal, K. Elucidation of the Functional Sulphur Chemical Structure in Asphaltenes Using First Principles and Deconvolution of Mid-Infrared Vibrational Spectra. *Fuel Process. Technol.* **2012**, *97*, 85–92. https://doi.org/10.1016/j.fuproc.2011.12.041.

(39) Castellano, O.; Gimon, R.; Soscun, H. Theoretical Study of the σ-π And π-π Interactions in Heteroaromatic Monocyclic Molecular Complexes of Benzene, Pyridine, and Thiophene Dimers: Implications on the Resin-Asphaltene Stability in Crude Oil. *Energy and Fuels* **2011**, *25* (6), 2526–2541. https://doi.org/10.1021/ef101471t.

(40) Da Costa, L. M.; Stoyanov, S. R.; Gusarov, S.; Tan, X.; Gray, M. R.; Stryker, J. M.; Tykwinski, R.; De M. Carneiro, J. W.; Seidl, P. R.; Kovalenko, A. Density Functional Theory Investigation of the Contributions of π-π Stacking and Hydrogen-Bonding Interactions to the Aggregation of Model Asphaltene Compounds. In *Energy and Fuels*; American Chemical Society, 2012; Vol. 26, pp 2727–2735. https://doi.org/10.1021/ef202010p.

(41) Eckart, C. The Penetration of a Potential Barrier by Electrons. *Phys. Rev.* **1930**, *35* (11), 1303–1309. https://doi.org/10.1103/PhysRev.35.1303.

(42) Geerlings, P.; De Proft, F.; Langenaeker, W. Conceptual Density Functional Theory. *Chem. Rev.* **2003**, *103* (5), 1793–1873. https://doi.org/10.1021/cr990029p.

(43) Mousavi, M.; Pahlavan, F.; Oldham, D.; Hosseinnezhad, S.; Fini, E. H. Multiscale Investigation of Oxidative Aging in Biomodified Asphalt Binder. *J. Phys. Chem. C* **2016**, *120* (31), 17224–17233. https://doi.org/10.1021/acs.jpcc.6b05004.

(44) Parr, R. G.; Pearson, R. G. Absolute Hardness: Companion Parameter to Absolute Electronegativity. *J. Am. Chem. Soc.* **1983**, *105* (26), 7512–7516. https://doi.org/10.1021/ja00364a005.

(45) Cárdenas, C.; Ayers, P.; De Proft, F.; Tozer, D. J.; Geerlings, P. Should Negative Electron Affinities Be Used for Evaluating the Chemical Hardness? *Phys. Chem. Chem. Phys.* **2011**, *13* (6), 2285–2293. https://doi.org/10.1039/c0cp01785j.

(46) Tozer, D. J.; De Proft, F. Computation of the Hardness and the Problem of Negative Electron Affinities in Density Functional Theory. *J. Phys. Chem. A* **2005**, *109* (39), 8923–8929. https://doi.org/10.1021/jp053504y.

(47) De Proft, F.; Sablon, N.; Tozer, D. J.; Geerlings, P. Calculation of Negative Electron Affinity and Aqueous Anion Hardness Using Kohn-Sham HOMO and LUMO Energies. In *Faraday Discussions*; Royal Society of Chemistry, 2007; Vol. 135, pp 151–159. https://doi.org/10.1039/b605302p.

(48) Koopmans, T. Über Die Zuordnung von Wellenfunktionen Und Eigenwerten Zu Den Einzelnen Elektronen Eines Atoms. *Physica* **1934**, *1* (1–6), 104–113. https://doi.org/10.1016/S0031-8914(34)90011-2.

(49) Ghanty, T. K.; Ghosh, S. K. Correlation between Hardness, Polarizability, and Size of Atoms, Molecules, and Clusters. *J. Phys. Chem.* **1993**, *97* (19), 4951–4953. https://doi.org/10.1021/j100121a015.

(50) Mirkin, C. A.; Ratner, M. A. Molecular Electronics. *Annu. Rev. Phys. Chem.* **1992**, *43* (1), 719–754. https://doi.org/10.1146/annurev.pc.43.100192.003443.

(51) Martín-Martínez, F. J.; Melchor, S.; Dobado, J. A. Clar- Kekulé Structuring in Armchair Carbon Nanotubes. *Org. Lett.* **2008**, *10* (10), 1991–1994. https://doi.org/10.1021/ol800587s.

(52) Martín-Martínez, F. J.; Melchor, S.; Dobado, J. A. Edge Effects, Electronic Arrangement, and Aromaticity Patterns on Finite-Length Carbon Nanotubes. *Phys. Chem. Chem. Phys.* **2011**, *13* (28), 12844–12857. https://doi.org/10.1039/c1cp20672a.

(53) Martín-Martínez, F. J.; Fias, S.; Van Lier, G.; De Proft, F.; Geerlings, P. Electronic Structure and Aromaticity of Graphene Nanoribbons. *Chem. - A Eur. J.* **2012**, *18* (20), 6183–6194. https://doi.org/10.1002/chem.201103977.

(54) Ye, X.; Li, Z. H.; Wang, W.; Fan, K.; Xu, W.; Hua, Z. The Parallel π-π Stacking: A Model Study with MP2 and DFT Methods. *Chem. Phys. Lett.* **2004**, *397* (1–3), 56–61. https://doi.org/10.1016/j.cplett.2004.07.115.

(55) Xu, W.; Chen, Y. F.; Hua, Z. Y. Imaging of Hydrogen Atoms and Stacks of Phenyl Groups on the Surface of Polystyrene Microparticles by Scanning Tunneling Microscopy. *J. Macromol. Sci. - Phys.* **1997**, *36* (3), 395–400. https://doi.org/10.1080/00222349708212392.

(56) Cai, W.; Xu, D.; Qian, L.; Wei, J.; Xiao, C.; Qian, L.; Lu, Z. Y.; Cui, S. Force-Induced Transition of Ï€-ΠStacking in a Single Polystyrene Chain. *J. Am. Chem. Soc.* **2019**, *141* (24), 9500–9503. https://doi.org/10.1021/jacs.9b03490.

(57) Beck, L.; Hägele, P. C. Semiempirical Atomistic Calculations of Kink Isomers in the Isotactic Polystyrene Chain. *Colloid Polym. Sci. Kolloid Zeitschrift Zeitschrift für Polym.* **1976**, *254* (2), 228–236. https://doi.org/10.1007/BF01517037.

(58) Singh, B.; Gupta, M.; Kumar, L. Bituminous Polyurethane Network: Preparation, Properties, and End Use. *J. Appl. Polym. Sci.* **2006**, *101* (1), 217–226. https://doi.org/10.1002/app.23198.

(59) Grinstaff, M. W.; Balijepalli, A. S.; McNeely, J. H.; Hamoud, A. Guidelines for β-Lactam Synthesis: Glycal Protecting Groups Dictate Stereoelectronics and [2+2] Cycloaddition Kinetics. *J. Org. Chem.* **2020**, *85* (19), 12044–12057. https://doi.org/10.1021/acs.joc.0c00510.

(60) Cossío, F. P.; Lecea, B.; Lopez, X.; Roa, G.; Arrieta, A.; Ugalde, J. M. An Ab Initio Study on the Mechanism of the Alkene–Isocyanate Cycloaddition Reaction to Form β-Lactams. *J. Chem. Soc., Chem. Commun.* **1993**, *0* (18), 1450–1452. https://doi.org/10.1039/C39930001450.

(61) Freitag, D.; Drees, M.; Goutal, S.; Strassner, T.; Metz, P. Synthetic and Computational Studies on Intramolecular [2+2] Sulfonyl Isocyanate-Olefin Cycloadditions. *Tetrahedron* **2005**, *61* (23), 5615–5621. https://doi.org/10.1016/j.tet.2005.03.075.

(62) Canto, L. B.; Mantovani, G. L.; Deazevedo, E. R.; Bonagamba, T. J.; Hage, E.; Pessan, L. A. Molecular Characterization of Styrene-Butadiene-Styrene Block Copolymers (SBS) by GPC, NMR, and FTIR. *Polym. Bull.* **2006**, *57* (4), 513–524. https://doi.org/10.1007/s00289-006-0577-4.

(63) Pacheco-Sánchez, J. H.; Zaragoza, I. P.; Martínez-Magadán, J. M. Asphaltene Aggregation under Vacuum at Different Temperatures by Molecular Dynamics. *Energy and Fuels* **2003**, *17* (5), 1346–1355. https://doi.org/10.1021/ef020226i.

Response to reviewer comments

REVIEWER 1

1. The keywords should be polished to well reflect the key points of this article.

Thank you for your comment. We have revised the key words to reflect the key take home messages (compatibilizing agent, increased phase stability) in this work, and make clearer the methods used (DFT, xTB, AFM).

2. Please explain that why the three asphaltene molecules (denoted as AS1, AS2, and AS3 in Figure 1a, b, c) are selected in this work.

Thank you for your comment – we have made modifications to the text to explain this selection in further detail. Please see a further detailed response below as well.

Asphalt is a complex fluid, and is very challenging to characterize. Thus, the development of asphaltene models has been a matter of discussion for many years. Describing the detail molecular structure of all the asphaltenes presented in an asphalt mixture is impossible. Therefore it has been commonly accepted to use some asphaltene molecules that describe on average the functional groups, molecular size, and chemical structure of asphalenes. According to experimental results, asphaltenes have aromatic cores of 4-6 aromatic rings, aliphatic chains of 6-12 carbon atoms in length and some heteroatom like S, N or O. There are some models of that suggest island-types of asphaltenes and other suggest archipelago-type. Michael Greenfield (ref 12-14) and Oliver Mullins (ref 15, 17) have been leading the modelling of asphaltenes. Both has proposed different models with different structures, always following the idea of representing the average. Finally, Mullins proposed an asphalt model with 12 molecules, including 3 asphaltenes, and this model, so-called Modified Yen-Mullins model (ref 17), has been accepted as a good standard for the average representation of asphalt. Michale Greenfield also adopted it, and Martin-Martinez improved it by including Clar Sextet Theory into the chemical structures proposition (ref 18). In summary, the selection of the asphaltenes has been made by adopting the commonly accepted average structures that described the countless number of asphaltene molecules in asphalt mixtures.

3. The mechanism behind the phenomenon should be discussed and analyzed deeply.

Thank you for your comment. A discussion of the mechanism behind the MDI stabilization of SBS and asphalt phases is present below and added to the conclusion.

We explored multiple mechanisms to explain this compatibilization phenomenon. From examining the electronic structure of additives stacked with asphaltenes, it was observed that MDI π–π stacks with asphaltenes while butadiene and styrene do not. This orbital interaction is expected to stabilize the MDI-asphaltene structure. However, the small difference between π–π stack distances of asphaltene cores when in the presence of MDI, butadiene, and styrene suggests that noncovalent π–π stacks contribute only minimally to the enhanced phase stability of SBS in asphalt when MDI is added. Instead, this compatibilizing effect is likely the result of

interactions of mostly covalent nature, through reactions between individual components. Our rate of reaction study supports the reaction of isocyanate with aromatics containing polar groups at the elevated mixing temperature of asphalt blends, which has already been studied and reported to take place. Most importantly, the rate of reaction study also supports the reaction of isocyanate with butadiene at the same elevated temperature, as hypothesized due to the ability for isocyanates to undergo cycloaddition reaction with the unsaturated groups in butadiene. The reaction of MDI with both aromatics and butadiene is a plausible mechanism for the role of MDI as a linkage between asphaltene and SBS phases in asphalt.

4. In my opinion, the conclusion should be listed one by one.

Thank you for your note. We have changed the structure to more clearly delineate the conclusions by listing them as first, second, and third.

REVIEWER 2

1. Are there any experimental pieces of evidence for the effects of temperature and mechanical loads on phase stability?

We have included some additional references to the effects of temperature on phase stability. A discussion of these references is below.

Regarding the effects of temperature on phase stability, Wen et. al baked SBS-modified asphalt at 163°C in an oven for 48 h and saw phase separation between the bottom and top thirds of the storage tube.[3] *In another study, Singh et. al examined SBS modified bitumen stored samples at 150 °C, 180 °C, and 210 °C for 3,7, and 21 days and saw that all the samples showed phase stability.*[2] *However, they crosslinked the polymer using 0.12% sulfur to prevent phase separation. Phase separation was also observed in the thermal loading of unmodified asphalt. Asphalt samples were rapidly heated to 50°C and then the temperature gradually decreased to 20°C by 3°C or 4°C intervals.*[4] *Two separate phases were observed. We did not find studies that isolate the effect of mechanical load on phase separation between the polymer additive and asphalt at ambient temperatures, so we have not included such references here. This is likely because diffusion or Brownian flocculation is often the main mechanism of gross phase separation.*[3]

2. A mixing rule (Eq. 7) is used to assess the phase stability, where entropic effects were neglected. Could the authors elaborate on the potential impact of such a simplification, especially as the results are discussed as a function of oligomer length?

This is a good point and we have included greater explanation of this in the manuscript. The use of this simple, and easily evaluated, mixing rule is supported by the fact that the entropy of mixing of a polymer blend is typically very nearly 0 or even slightly negative. This is particularly true for significant degrees of polymerization, as would certainly be the case for commercial SBS and oligomeric MDI. Therefore, the contribution of entropic effects to the free energy of mixing would be negligible or slightly positive. Therefore, the mixing energy (as estimated with equation 7), or enthalpy, would be the dominant contributor to the free energy. Furthermore, application of equation 7 to oligomers (from two to six monomeric units) of

polyphenylene oxide (PPO) and polystyrene result in negative mixing energies within the currently employed methodology (results not reported). These two polymers are well known to form a compatible, single-phase blend with a single glass transition temperature.

3. What does '0' in Table 4 means? What is the criterion of 'low rate'? Could the authors add more discussions on the systematic errors of 2-3 orders of magnitude in the reaction rates? Is it relevant for the diffusive process that may limit the rate of reaction?

The computed values of the reaction rate constant for the forward and reverse reactions of phenol and carbazole at 30ºC, and the reverse reaction of cis-2-butene were less than 10^{-18} l/mol/hr. Therefore, in the table, we incorrectly approximated the values as zero. As such, we have amended the table to replace "0" in Table 4 with "less than 10^{-18}".

Regarding the systematic errors of 2-3 orders of magnitude, as a result of the many approximations inherent in the DFT calculations of the kinetic rate constants (basis set size, exchange-correlation function used, simplified tunneling correction, approximate treatment of solvation, etc.) an exact agreement between experiment and theory is difficult to obtain. This is exacerbated by the exponential dependence of the rate constant on the energetic barrier height. Therefore, the employed strategy to obtain reliable results was to treat all studied reactions at the same level of theory and to apply systematic corrections from a comparison to experiments. We have amended the text to include a greater discussion of these systematic errors.

We thank the reviewer for this very valid point regarding the diffusive process that may limit the rate of the reaction. The high viscosities of the asphalt blends can certainly limit the reaction rates due to mass transfer limitations. Nonetheless, given the high temperature, long reaction times and aggressive mixing of the components, we suggest that the reactions can take place at a reasonable rate. We have incorporated this discussion of viscosity into the main text.